Common variable immunodeficiency–associated endotoxemia promotes early commitment to the T follicular lineage

Carole Le Coz, PhD,[a] Bertram Bengsch, MD, PhD,[h] Caroline Khanna, BA,[a] Melissa Trofa, BA,[a] Takuya Ohtani, PhD,[g] Brian E. Nolan, MD,[c] Sarah E. Henrickson, MD, PhD,[a,d,g] Michele P. Lambert, MD,[b,d] Taylor Olmsted Kim, MD,[i] Jenny M. Despotovic, DO,[i] Scott Feldman, MD, PhD,[e] Olajumoke O. Fadugba, MD,[e] Patricia Takach, MD,[e] Melanie Ruffner, MD, PhD,[a] Soma Jyonouchi, MD,[a,d] Jennifer Heimall, MD,[a,d] Kathleen E. Sullivan, MD, PhD,[a,d,g] E. John Wherry, PhD,[f,g] and Neil Romberg, MD[a,d,g]

Philadelphia, Pa, Freiburg, Germany, and Houston, Tex

GRAPHICAL ABSTRACT

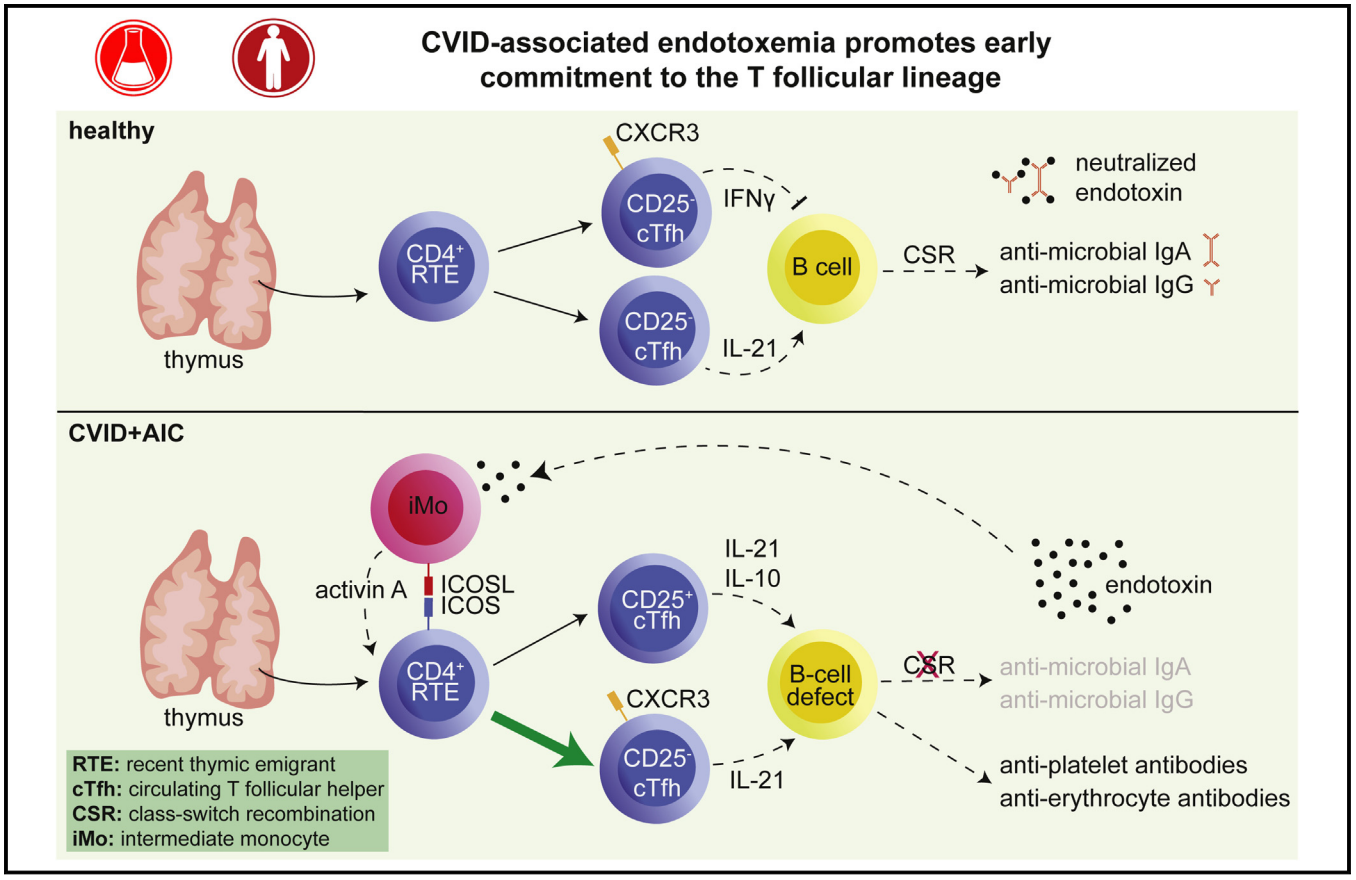

From the Divisions of [a]Immunology and Allergy, [b]Hematology, and [c]Rheumatology, Children's Hospital of Philadelphia; the Departments of [d]Pediatrics and [e]Medicine, Division of Allergy and Immunology, [f]Systems Pharmacology and Translational Therapeutics, and [g]the Institute for Immunology, Perelman School of Medicine at the University of Pennsylvania, Philadelphia; [h]the Department of Medicine II, University Medical Center Freiburg; and [i]the Department of Pediatrics, Hematology/Oncology Section, Baylor College of Medicine, Houston.

Supported by grant numbers K23AI115001 (to N.R.), AI146026 (to N.R.), AI105343 (to E.J.W.), AI108545 (to E.J.W.), and AI117950 (to E.J.W.) from the National Institutes of Health/National Institute of Allergy and Infectious Diseases; grant CA210944 from the National Institutes of Health/National Cancer Institute (to E.J.W.); grant number K12HD043245 from the National Institutes of Health/National Institute of Child Health and Human Development (to S.E.H.); the American Association of Allergy, Asthma & Immunology Foundation (to S.E.H.); the David and Hallee Adelman Immunotherapy Research Fund (to E.J.W.); the Parker Institute for Cancer Immunotherapy Bridge Scholar Award to (E.J.W.); and the Jeffrey Modell Foundation (to N.R.).

Disclosure of potential conflict of interest: E. J. Wherry is a member of the Parker Institute for Cancer Immunotherapy which supported the UPenn cancer immunotherapy program; has consulting agreements with and/or is on the scientific advisory board for Merck, Roche, Pieris, Elstar, and Surface Oncology; is a founder of Arsenal Biosciences; and has a patent licensing agreement on the PD-1 pathway with Roche/Genentech. The rest of authors declare that they have no relevant conflicts of interest.

Received for publication April 12, 2019; revised July 26, 2019; accepted for publication August 5, 2019.

Corresponding author: Neil Romberg, MD, Children's Hospital of Philadelphia, Abramson Research Center, Rm 1216C, Philadelphia, PA 19104. E-mail: rombergn@email.chop.edu.

0091-6749/$36.00

https://doi.org/10.1016/j.jaci.2019.08.007

Background: Although chiefly a B-lymphocyte disorder, several research groups have identified common variable immunodeficiency (CVID) subjects with numeric and/or functional T_H cell alterations. The causes, interrelationships, and consequences of CVID-associated $CD4^+$ T-cell derangements to hypogammaglobulinemia, autoantibody production, or both remain unclear.

Objective: We sought to determine how circulating $CD4^+$ T cells are altered in CVID subjects with autoimmune cytopenias (AICs; CVID+AIC) and the causes of these derangements.

Methods: Using hypothesis-generating, high-dimensional single-cell analyses, we created comprehensive phenotypic maps of circulating $CD4^+$ T cells. Differences between subject groups were confirmed in a large and genetically diverse cohort of CVID subjects (n = 69) by using flow cytometry, transcriptional profiling, multiplex cytokine/chemokine detection, and a suite of *in vitro* functional assays measuring naive T-cell differentiation, B-cell/T-cell cocultures, and regulatory T-cell suppression.

Results: Although $CD4^+$ T_H cell profiles from healthy donors and CVID subjects without AICs were virtually indistinguishable, T cells from CVID+AIC subjects exhibited follicular features as early as thymic egress. Follicular skewing correlated with IgA deficiency–associated endotoxemia and endotoxin-induced expression of activin A and inducible T-cell costimulator ligand. The resulting enlarged circulating follicular helper T-cell population from CVID+AIC subjects provided efficient help to receptive healthy donor B cells but not unresponsive CVID B cells. Despite this, circulating follicular helper T cells from CVID+AIC subjects exhibited aberrant transcriptional profiles and altered chemokine/cytokine receptor expression patterns that interfered with regulatory T-cell suppression assays and were associated with autoantibody production.

Conclusions: Endotoxemia is associated with early commitment to the follicular T-cell lineage in IgA-deficient CVID subjects, particularly those with AICs. (J Allergy Clin Immunol 2019;■■■:■■■-■■■.)

Key words: *Common variable immunodeficiency, autoimmune cytopenias, activin A, endotoxin, follicular helper T cell, regulatory T cell, recent thymic emigrant, time-of-flight cytometry*

Abbreviations used

AIC:	Autoimmune cytopenia
AIHA:	Autoimmune hemolytic anemia
CFSE:	Carboxyfluorescein diacetate succinimidyl ester
CSR:	Class-switch recombination
cT_{FH}:	Circulating follicular helper T
CVID:	Common variable immunodeficiency
CVID+AIC:	CVID subjects with AICs
CVID−AIC:	CVID subjects without AICs
CyTOF:	Time-of-flight cytometry
ES:	Evans syndrome
FACS:	Fluorescence-activated cell sorting
FOXP3:	Forkhead box P3
HD:	Healthy donor
ICOS:	Inducible T-cell costimulator
ICOSL:	Inducible T-cell costimulator ligand
ITP:	Immune thrombocytopenia
PD-1:	Programmed cell death protein 1
RTE:	Recent thymic emigrant
T_{FH}:	Follicular helper T
TLR:	Toll-like receptor
Treg:	Regulatory T
t-SNE:	t-Distributed Stochastic Neighbor Embedding

Common variable immunodeficiency (CVID) subjects are antibody deficient, and approximately 20% experience autoantibody-mediated autoimmune cytopenias (AICs).[1] Several lines of evidence suggest CVID is chiefly caused by B-cell dysfunction. CVID B cells display an array of impairments, including defective tolerance,[2,3] diminished Toll-like receptor (TLR) 7/9 signaling,[4,5] absent thymus-independent antibody responses,[6] curtailed class-switch recombination (CSR),[7] somatic hypermutation,[8-10] blocked plasma cell differentiation,[11] and IgG/IgA deficiency–associated endotoxemia.[8,12] Additionally, most monogenic forms of CVID are linked to genes critical to B cell–centric pathways, including early B-cell development,[13] the B-cell activating factor/a proliferation-inducing ligand axis,[3,14-16] B-cell receptor signal transduction,[17-19] B-cell costimulation,[20,21] and terminal B-cell differentiation.[22]

Despite the central role of B lymphocytes in CVID pathogenesis, disease-associated alterations in several $CD4^+$ T-cell subsets have been reported, including diminished numbers of recent thymic emigrants (RTEs),[23-25] poorly suppressive regulatory T (Treg) cells,[3,8,26] and increased frequencies of circulating follicular helper T (cT_{FH}) cells.[3,8,27] The causes, interrelationships, and consequences of CVID-associated $CD4^+$ T-cell derangements to hypogammaglobulinemia and/or autoantibody production remain unclear.

To more wholly capture CVID T_H cell landscapes, we compared high-dimensional single-cell analyses of peripheral blood samples from CVID subjects and healthy donors (HDs). Although the $CD4^+$ T-cell profiles of CVID subjects without AICs (CVID−AIC) were indistinguishable from those of HD control subjects, we report here that T_H profiles of CVID subjects with AICs (CVID+AIC) possess a pervasive follicular signature. We further demonstrate the direct and indirect effects of systemic endotoxemia favor commitment to the follicular helper T (T_{FH}) cell lineage as early as thymic egress. This results in enlarged circulating T_{FH} cell pools that express aberrant chemokine and cytokine receptors. In total, our data provide a unifying inflammatory framework connecting seemingly disparate CVID-associated T-cell subset alterations to IgA deficiency–associated endotoxemia.

METHODS

Human samples

Peripheral blood samples from 69 subjects with (17 subjects) and without AICs (52 subjects; see Table E1 in this article's Online Repository at www.jacionline.org) were obtained by using standard phlebotomy. Each CVID subject met the 1999 Pan-American Group for Immunodeficiency CVID diagnostic criteria[28] at the time of enrollment, and all were receiving antibody replacement therapy. None were receiving chronic immunomodulatory therapy at enrollment. We defined immune thrombocytopenia (ITP) using established clinical criteria.[29-31] Autoimmune hemolytic anemia (AIHA) was

defined by a hemoglobin level of less than 11 g/dL, evidence of hemolysis, and a positive direct antibody test result. Subjects with negative direct antibody test results with hemolysis were also considered to have AIHA if other acquired and hereditary forms of hemolytic anemia were excluded.[32,33] Evans syndrome (ES) was defined as those meeting both AIHA and ITP diagnostic criteria simultaneously or sequentially within at most a 10-year-period. The average age of enrolled CVID+AIC subjects was 23.9 years (range, 4-57 years); 58.8% were male. Genotyping of CVID subjects was performed at genes listed by the International Union of Immunologic Societies to be associated with primary immune deficiencies.[34] The average age of enrolled CVID−AIC subjects was 18.8 years (range, 3-60 years); 50.0% were male. We also analyzed peripheral blood samples from 33 related and unrelated HD control subjects with a mean age of 25.2 years (range, 4-59 years); 42.2% were male. As an additional comparator, we analyzed peripheral blood samples from a cohort of 14 immunocompetent subjects with AICs comprised of 12 subjects with ITP and 2 subjects with ES. Their mean age was 14.1 years (range, 3-18 years); 36% were male. Study protocols were approved by the institutional review boards of Children's Hospital of Philadelphia, the University of Pennsylvania, and Baylor College of Medicine.

Mass cytometry

Mass cytometry reagents were obtained or generated by using custom conjugation to isotope-loaded polymers by using MAXPAR kits (Fluidigm, South San Francisco, Calif). Antibodies for mass cytometry were chosen to target 38 molecules relevant to $CD4^+$ T-cell biology, including chemokine receptors, transcription factors, cell-cycle antigens, and activating/inhibitory immunoreceptors (see Table E2 in this article's Online Repository at www.jacionline.org).

Cell staining was performed, as previously described.[35] Briefly, circulating $CD4^+$ T cells from 3 CVID−AIC subjects, 3 CVID+AIC subjects, and 3 sex- and age-matched HDs were purified by using the MojoSort Human CD4 T Cell Isolation Kit (BioLegend, San Diego, Calif). Circulating $CD4^+$ T cells (2×10^6) were then stained with 20 μmol/L L/D-139 for 10 minutes at room temperature for live/dead cell discrimination. Cells were washed in PBS with 1% FBS. After incubation with a surface antibody cocktail for 30 minutes at room temperature, cells were fixed and permeabilized with the FOXP3/Transcription Factor Staining Buffer Set (eBioscience, Carlsbad, Calif) before intracellular staining. Cells were further fixed in 1.6% paraformaldehyde (Electron Microscopy Sciences, Hatfield, Pa) solution containing 125 nmol/L iridium overnight at 4°C and characterized by using mass cytometry with a CyTOF Helios instrument (Fluidigm). Bead-based normalization of time-of-flight cytometry (CyTOF) data was performed by using the Nolan Lab Normalizer (https://github.com/nolanlab/bead-normalization/releases). Analyses of individual subject samples from the same clinical group were pooled and then reduced into 2-dimensional t-Distributed Stochastic Neighbor Embedding (t-SNE) plots.[36] Cell clustering was performed with self-organizing map software (FlowSOM; https://github.com/SofieVG/FlowSOM).[37] HD and CVID+AIC clusters containing 4-fold or greater cell number differences were chosen for downstream analyses.

Cell preparation, flow cytometry, and cell sorting

PBMCs were isolated from peripheral blood samples by using Ficoll-Paque PLUS density gradient centrifugation (GE Healthcare Life Sciences, Chicago, Ill). Cells were surface antibody stained (see Table E3 in this article's Online Repository at www.jacionline.org) and, when appropriate, fixed and permeabilized for intracellular staining. Cells were analyzed with an LSRFortessa (BD Bioscience, San Jose, Calif) and/or sorted with a MoFlo Astrios EQ (Beckman Coulter, Fullerton, Calif). Fluorescence-activated cell sorting (FACS) data were visualized with FlowJo software (TreeStar, Ashland, Ore). For cytokine staining, mononuclear cells were rested overnight at 37°C, followed by 6 hours of stimulation with phorbol 12-myristate 13-acetate (25 ng/mL; Sigma, St Louis, Mo) and ionomycin (1 μg/mL; Sigma) in the presence of brefeldin A (5 μg/mL; BD Biosciences). After activation, cells were incubated with a surface antibody cocktail for 30 minutes at room temperature and then fixed, permeabilized, and intracellularly stained. All antibodies used for FACS analyses are listed in Table E3.

In vitro naive $CD4^+$ T-cell activation

Batch-sorted $CD4^+CD45RO^-$ HD naive $CD4^+$ T cells were plated at 100,000 cells/well with anti-CD2/CD3/CD28–coated beads (Miltenyi Biotec, Bergisch Gladbach, Germany) in the presence of the subject's plasma (20%) or FBS (20%). After 24 hours, cells, beads, and plasma/FBS-containing media were transferred to a recombinant inducible T-cell costimulator ligand (ICOSL)−coated plate (5 μg/mL; R&D Systems, Minneapolis, Minn). On culture day 5, cells were analyzed for CXCR5 and programmed cell death protein 1 (PD-1) expression by using FACS. In some cases 50 μg/mL polymyxin B (InvivoGen, San Diego, Calif) was added to plasma samples from CVID+AIC subjects, or FBS was spiked with LPS (100 ng/mL; Sigma) on culture day 0.

T-cell/B-cell cocultures

$CD19^+CD21^+CD27^-IgM^+$ sorted naive B cells or $CD19^+CD21^+CD27^+$ sorted memory B cells (2.5×10^4) were cocultured with an equal number of $CD4^+CD45RO^+CD25^-CD127^+CXCR5^+PD\text{-}1^+$ sorted cT_{FH} cells. Cocultures were activated by addition of anti-CD2/CD3/CD28–coated beads at a ratio of 1 bead per T cell. On culture day 7, the frequency of surface IgG-, IgA-, and CD38-expressing B cells was measured by using FACS. Culture supernatant IgM, IgG, and IgA concentrations were determined by using an ELISA. In some cocultures naive B cells were stained with carboxyfluorescein diacetate succinimidyl ester (CFSE; Thermo Fisher Scientific, Waltham, Mass) to determine proliferative responses.

In vitro Treg cell suppression assay

$CD4^+CD45RO^-CD127^+CD25^-$ sorted naive responder T cells (5×10^3) were labeled with CFSE and cocultured with an equal number of either $CD4^+CD25^{hi}CD127^{lo/-}$ "all," $CD4^+CD25^{hi}CD127^{lo/-}CXCR5^-$ "Treg," or $CD4^+CD25^{hi}CD127^{lo/-}CXCR5^+PD\text{-}1^{hi}CD25^{hi}$ "cT_{FH}" cells. Cultures were activated with anti-CD2/CD3/CD28−coated beads. Cocultures were stained for viability with the LIVE/DEAD Kit (Thermo Fisher Scientific), and the proliferation of viable responder T cells was determined by using CFSE dilution at culture day 3.5 to 4.5 with FACS.

Cytokine, chemokine, and immunoglobulin quantification

Cytokine and chemokine concentrations were measured in thawed plasma using Milliplex (T-cell panel; Millipore-Sigma, Burlington, Mass) and LEGENDplex (human proinflammatory chemokine panel; BioLegend). Activin A plasma concentrations and IgG, IgA, and IgM supernatant concentrations were measured by using ELISAs (R&D Systems and Jackson ImmunoResearch [West Grove, Pa], respectively). Serum immunoglobulin isotype concentrations were determined by the clinical immunology laboratories at the Children's Hospital of Philadelphia and the University of Pennsylvania.

Gene expression microarrays

$CD4^+CD25^-CD127^+CXCR5^+PD\text{-}1^{hi}CXCR3^+$ and $CD4^+CD25^-CD127^+CXCR5^+PD\text{-}1^{hi}CXCR3^-$ cells from 3 HDs and $CD4^+CD25^-CD127^+CXCR5^+PD\text{-}1^{hi}$ cells from 4 CVID+AIC subjects were FACS sorted. RNA was isolated by using the Direct-zol RNA MicroPrep (Zymo Research, Irvine, Calif), and transcriptional profiles were determined by using the Clarion S Pico Array (Affymetrix, Santa Clara, Calif), according to the manufacturer's instructions.

Differentially expressed transcripts were subjected to hierarchical clustering (Affymetrix console) and gene set enrichment analysis with the Molecular Signatures Database, version 6.2 (http://software.broadinstitute.org/gsea/index.jsp).[38,39]

Statistics

Data were analyzed with GraphPad Prism software (GraphPad Software, La Jolla, Calif) by using either Mann-Whitney *U*, paired Student *t*, or Pearson correlation coefficient tests.

RESULTS

Activated and follicular features predominate in T_H cell landscapes from CVID+AIC subjects

From a large and genetically diverse CVID cohort (n = 69; see Table E1), we chose 3 representative subjects with AICs, 3 without AICs, and 3 age- and sex-matched HD control subjects for high-dimensional T_H cell analyses. All 3 CVID+AIC subjects lacked detectable serum IgA; they included a 57-year-old female with ITP carrying a heterozygous W783X NFKB1 variant, a 30-year-old male with both ES and granulomatous lymphocytic interstitial lung disease carrying a heterozygous C172Y TACI variant, and a 15-year-old male with ES but no identifiable mutations in CVID-associated genes. All 3 CVID−AIC subjects possessed detectable, although decreased, serum IgA concentrations (mean, 9 mg/dL). All HD control subjects were IgA replete.

To catalogue the phenotypic differences between these subjects' circulating $CD4^+$ T lymphocytes, we stained them with a custom panel of 38 heavy metal–conjugated antibodies targeting activation markers, chemokine receptors, inhibitory proteins, transcription factors, and cell-cycle proteins (see Table E2). Stained cells were analyzed by using mass cytometry or time-of-flight cytometry (CyTOF) to produce high-dimensional data sets that we subsequently reduced into 2-dimensional t-SNE plots.[36] Some markers were expressed more ubiquitously, whereas others were expressed only by distinct clusters of T_H cells (see Fig E1 in this article's Online Repository at www.jacionline.org).

Because plots within subject groups displayed similarities (see Fig E2 in this article's Online Repository at www.jacionline.org), we pooled them and scrutinized each group's plot with self-organizing map software that ignores *a priori* assumptions about T-cell biology (see Fig E3 in this article's Online Repository at www.jacionline.org).[37] Using this hypothesis-generating strategy, we found that pooled $CD4^+$ T-cell t-SNE plots for HDs and CVID−AIC subjects were virtually indistinguishable, whereas plots for CVID+AIC subjects displayed unique T-cell distribution patterns (Fig 1, *A*, left) that were concentrated in 3 spatially discrete populations (P1, P2, and P3; Fig 1, *A*, right). In samples from CVID+AIC subjects, the frequency of cells belonging to P1 (2.1%) was clearly diminished compared with that belonging to CVID−AIC subjects (29.6%) and HD P1 frequencies (27.3%), with redistribution into P2 (27.8%) and P3 (5.2%). Only 1.3% to 2.2% of $CD4^+$ cells from CVID−AIC subjects and HDs belonged to P2, and only 0.5% to 1.1% belonged to P3.

To determine identifying features of P1, P2, and P3, we first mapped conventional markers of naive T cells ($CD45RA^+CD45RO^-$) onto our t-SNE plots (green; Fig 1, *B*, left). In samples from HDs and CVID−AIC subjects, 41.6% to 51% of naive T cells belonged to P1, with the remaining cells belonging to a phenotypically related population (P1′). P1′ cells were distinct from P1 cells through expression of activation markers associated with follicular T-cell development, including CCR7, T-cell factor 1, CD38, and inducible T-cell costimulator (ICOS) expression (Fig 1, *B*, right, and see Fig E1).[40,41] Instead of belonging to P1, most naive T_H cells from CVID+AIC subjects mapped to P1′ (49.7%) and, to a lesser extent, P2 (10.3%). Like P1′, naive P2 cells expressed CCR7, T-cell factor 1, CD38, and ICOS but additionally expressed CXCR5 and PD-1, suggesting greater follicular commitment (Fig 1, *B*, right, and see Fig E1).[42-44]

Given the observed follicular skewing of naive T_H cells from CVID+AIC subjects, we next mapped the canonical T_{FH} surface markers CXCR5 and PD-1 onto t-SNE plots (Fig 1, *C*, left). Of T_H cells from CVID+AIC subjects, 85.9% expressing these markers belonged to P2. As mentioned above, some P2 cells were naive, but most (>90%) expressed CD45RO. Although scarce in samples from HDs/CVID−AIC subjects and abundant in samples from CVID+AIC subjects, $CXCR5^+PD\text{-}1^+$ cells from all 3 subject groups appeared phenotypically similar, except cells from CVID+AIC subjects expressed more ICOS, CXCR3, and T-cell immunoreceptor with immunoglobulin and ITIM domains but less CCR6 (Fig 1, *C*, right). Although absent in HDs and CVID−AIC subjects, 12.8% of $CXCR5^+PD\text{-}1^+$ cells from CVID+AIC subjects expressed the IL-2 receptor α chain (CD25; see Fig E4 in this article's Online Repository at www.jacionline.org), a surface marker categorically absent in *bona fide* T_{FH} cells from secondary lymphoid tissues.[45] In blood samples from CVID+AIC subjects, these CD25-expressing follicular cells primarily localized to P3.

CD25 expression by HD T_H cells denotes an activated or regulatory phenotype, whereas IL-7 receptor (CD127) coexpression excludes forkhead box P3 $(FOXP3)^+$ Treg cells.[46] Because FOXP3 staining requires fixation and permeabilization, the $CD25^{hi}CD127^{lo/-}$ "Treg" cell sorting gate has historically been used to isolate viable human Treg cells, including Treg cells from CVID subjects,[3,8,26] for *in vitro* suppression assays. To compare phenotypic diversity within the traditional "Treg" cell gate of CVID subjects, we mapped CD25 expression and CD127 low/nonexpression onto our t-SNE plots (Fig 1, *D*, left). We found a substantially increased proportion of $CD25^{hi}CD127^{lo/-}$ cells belonged to P3 in samples from CVID+AIC subjects (21.7%), whereas this distribution pattern was rare in samples from HDs (3.9%) and CVID−AIC subjects (3.3%). Compared with $CD25^{hi}CD127^{lo/-}$ cells from CVID+AIC subjects lying outside P3 ("Treg"-P3), those belonging to P3 expressed lower amounts of regulatory transcription factors (FOXP3 and Helios) but greater amounts of classical T_{FH} cells (ICOS, CXCR5, and PD-1) and activation/cell-cycle markers (CD95 and Ki67; Fig 1, *D*, right, and see Fig E1). Hence the T_H cell landscape in CVID+AIC subjects demonstrates unique features, including naive T-cell activation, prominent follicular skewing, and the presence of a uniquely expanded population possessing some features that are characteristic of Treg cells ($CD25^{hi}CD127^{lo/-}$) but others that are not ($FOXP3^{lo/-}CXCR5^+PD\text{-}1^{hi}Ki67^+$).

Endotoxemia favors early-stage follicular differentiation

To confirm and further explore the T-cell alterations observed in our CyTOF analysis, we analyzed peripheral blood samples from our full subject cohort (see Table E1) and age/sex-matched cohorts of immunocompetent subjects with AICs and HD control subjects by using standard flow cytometry (FACS). We first turned

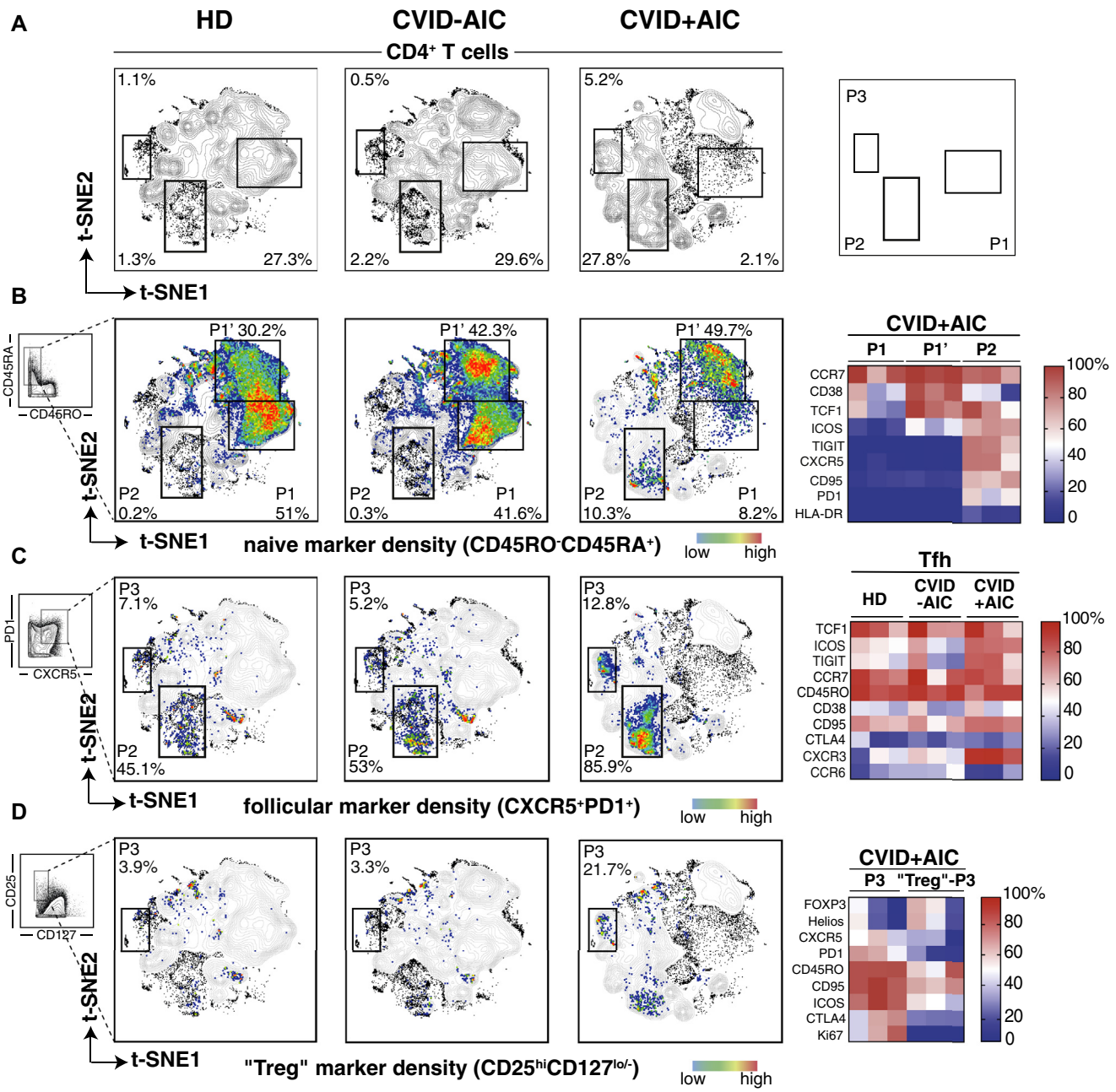

FIG 1. High-dimensional analyses of circulating $CD4^+$ T cells from CVID+AIC subjects reveal distinct distribution patterns and pervasive follicular signatures. **A,** Thirty-eight-dimension mass cytometric analyses of HDs (n = 3), CVID−AIC subjects (n = 3), and CVID+AIC subjects (n = 3) peripheral blood $CD4^+$ T cells are pooled and reduced into 2-dimensional t-SNE plots *(left)*. Between plots, cell distribution differences are concentrated into 3 spatially distinct populations: P1, P2, and P3. **B-D,** Density of cells coexpressing surface markers indicative of naive cells (Fig 1, *B*), T_{FH} cells (Fig 1, *C*), and "Treg" cells (Fig 1, *D*) in HDs are overlaid on ungated t-SNE plots. Heat maps compare the frequencies of cells from different populations expressing the indicated markers. Compared populations include naive cells belonging to P1, P2, or a third $CD45RA^+CD45RO^-$ population (P1′; Fig 1, *B*); cT_{FH} cells from each subject by group (Fig 1, *C*); and cells in the "Treg" cell gate belonging to P3 and not (Fig 1, *D*).

our attention to naive ($CD45RA^+CD45RO^-$) T_H cells, which comprised an average of 56.6% of $CD4^+$ cells from HDs, 54.4% of $CD4^+$ cells from immunocompetent subjects with AICs, and 58.1% of $CD4^+$ cells from CVID−AIC subjects but only 23.1% of cells from CVID+AIC subjects ($P < .0001$ for each comparison, see Fig E5 in this article's Online Repository at www.jacionline.org). As suggested by our CyTOF analyses, a small percentage of naive T_H cells from CVID+AIC subjects, but not cells from other subjects, coexpressed CXCR5 and PD-1 (mean, 4.7%; see Fig E6 in this article's Online Repository at www.jacionline.org). Diminishment of the naive T_H cell pool from CVID+AIC subjects was primarily caused by a 2-fold

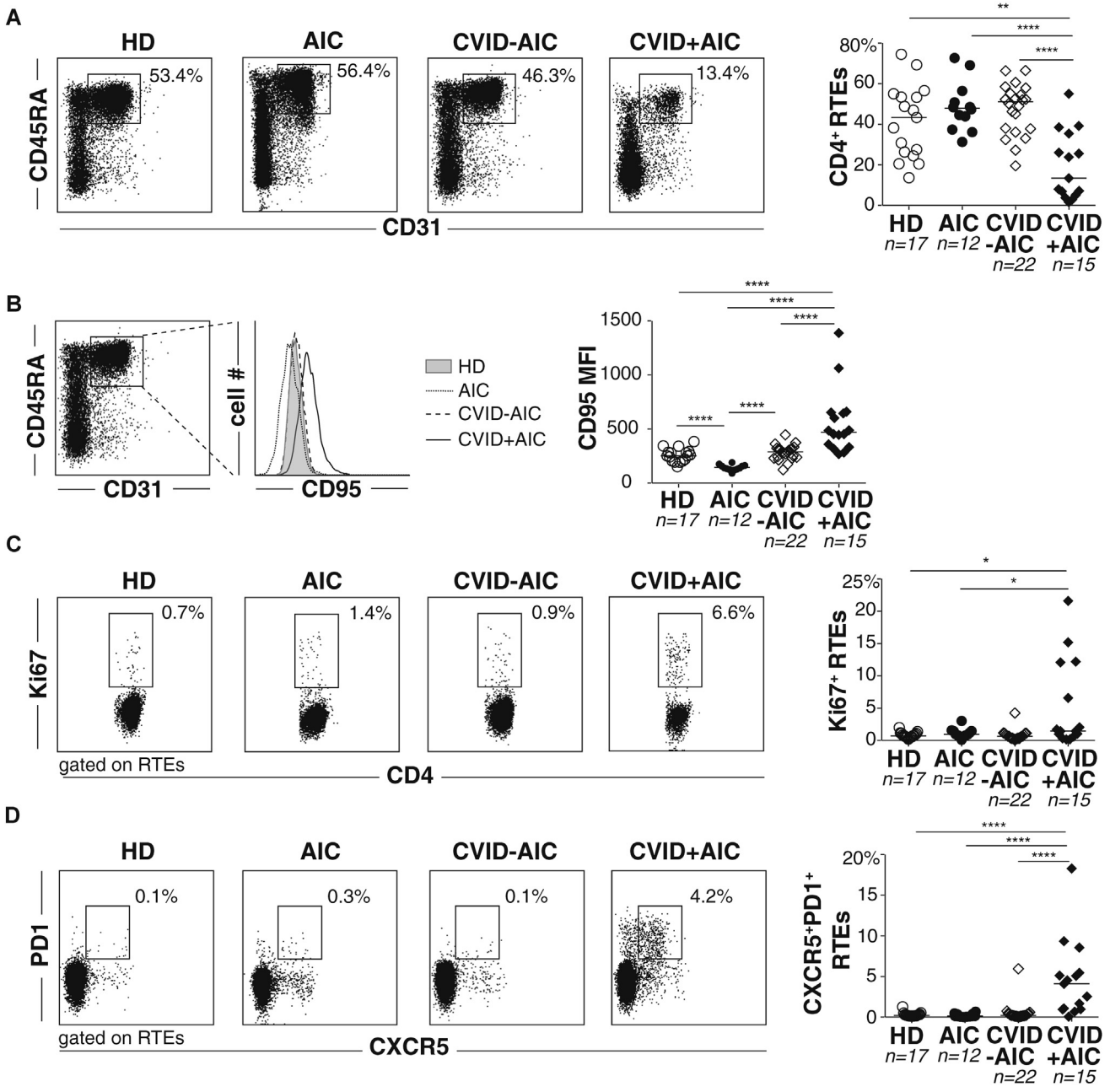

FIG 2. CD4$^+$ RTEs from CVID+AIC subjects express activation and follicular markers. **A,** Frequencies of RTEs among total CD4$^+$ T cells are displayed for representative subjects *(left)* and all available subjects. **B-D,** Comparison of CD95 expression intensities (Fig 2, *B*) and Ki67 and CXCR5 (Fig 2, *C*) and PD-1 (Fig 2, *D*) expression frequencies on CD4$^+$ RTEs from representative *(left)* and all available HDs, immunocompetent subjects with AICs, CVID−AIC subjects, and CVID+AIC subjects. **P* < .05, ***P* < .01, and *****P* < .0001, Mann-Whitney *U* test.

relative decrease in numbers of CD45RA$^+$CD31$^+$ RTEs (Fig 2, *A*),[47] a reduction not observed in the CD8 compartment (see Fig E7 in this article's Online Repository at www.jacionline.org). Although scarce, a significantly greater fraction of CD4$^+$ RTEs from CVID+AIC subjects expressed activation (CD95), cell-cycle (Ki67), and follicular (CXCR5 and PD-1) molecules than counterparts from CVID−AIC subjects and HD control subjects (Fig 2, *B-D*). Thus as early as thymic egress, T_H cells from CVID+AIC subjects display signs of activation, proliferation, and T_{FH} cell differentiation.

T_{FH} cell differentiation requires naive T_H cells and antigen-presenting cells to interact through soluble factors (IL-12, IL-6, and activin A)[48-50] and cell-cell contacts (T-cell receptor–MHC class II and ICOS-ICOSL).[51] To determine whether serum soluble factors contribute to the observed follicular skewing of T_H cells from CVID+AIC

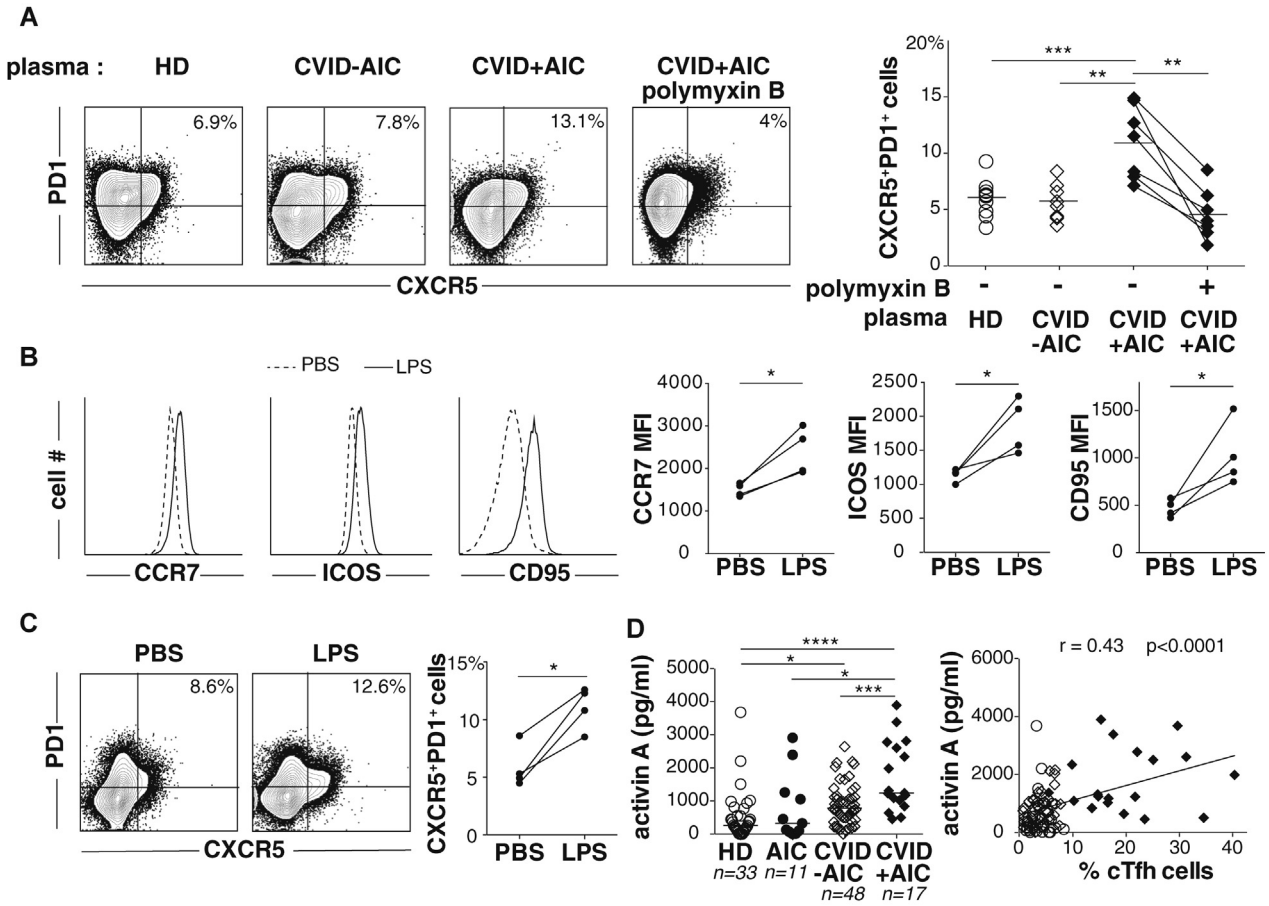

FIG 3. Endotoxemia promotes T_{FH} cell differentiation. **A,** Day 5 CXCR5/PD-1 coexpression on $CD45RO^-$ naive cells from HDs cultured with anti-CD3/CD28 beads, recombinant ICOSL, and 20% plasma from HDs, CVID−AIC subjects, or CVID+AIC subjects with and without polymyxin B. **B** and **C,** Day 2 CCR7, ICOS, and CD95 expression (Fig 3, *B*) and day 5 CXCR5 and PD-1 expression (Fig 3, *C*) on activated $CD45RO^-$ cells from HDs similarly cultured but in 20% FBS spiked with LPS (100 ng/mL) or not. *MFI,* Mean fluorescence intensity. **D,** Activin A plasma concentrations between groups and against paired cT_{FH} cell frequencies are displayed. $*P < .05$, $**P < .01$, $***P < .001$, and $****P < .0001$, Mann-Whitney *U* test or paired Student *t* test or Pearson correlation coefficient.

subjects, we cultured naive $CD4^+$ T cells from HDs with anti-CD2/CD3/CD28 beads, recombinant ICOSL, and plasma from either HDs, CVID−AIC subjects, or CVID+AIC subjects. After 5 days, an average of 6% of cells exposed to plasma from HDs and 5.7% exposed to plasma from CVID−AIC subjects coexpressed CXCR5 and PD-1. When the same HD cells were cultured with plasma from CVID+AIC subjects, the coexpression frequency increased significantly to 11% ($P < .01$ and $P < .001$, respectively; Fig 3, *A*). In all cases $CXCR5^+PD\text{-}1^+$ cells expressed more BCL6, the master T_{FH} transcriptional regulator, and more OX40, an important amplifier of T_{FH} cell development,[52] than $CXCR5^-PD\text{-}1^-$ cells from the same cultures (see Fig E8 in this article's Online Repository at www.jacionline.org).

Recently, we reported that most CVID+AIC subjects, including many analyzed here, possess undetectable serum IgA concentrations and varying degrees of endotoxemia.[8] To determine whether plasma endotoxin from CVID+AIC subjects skews T-cell development, we neutralized it with polymyxin B and repeated *in vitro* T_{FH} cell differentiation experiments. At day 5, CXCR5/PD-1 coexpression frequencies decreased precipitously in polymyxin B–containing cultures (4.6% vs 11%, $P < .01$; Fig 3, *A*).

To confirm this effect was due to LPS neutralization, we again T_{FH} differentiated naive T_H cells from HDs in culture but replaced subjects' plasma with LPS-spiked FBS (0.5 μg/mL). After 2 days of LPS exposure, cells began expressing the characteristic P1′ cell-surface markers CCR7, CD95, and ICOS (Fig 3, *B*). After 5 days of LPS exposure, cells from HDs coexpressed CXCR5 and PD-1 at a frequency similar to cells cultured in plasma from CVID+AIC subjects (Fig 3, *C*). Thus the endotoxin contained within plasma from CVID+AIC subjects directly promotes follicular molecule expression by $CD4^+$ T cells *in vitro*.

The inflammatory consequences of endotoxemia are diverse but include myeloid lineage cell release of inflammatory cytokines, including the powerful inducer of T_{FH} cell differentiation activin A.[50,53] To determine whether chronic CVID-related endotoxemia was associated with greater activin A release, we measured its concentration in subjects' plasma. Indeed, the average activin A concentrations were much greater in samples from CVID+AIC subjects (1722 pg/mL) than in

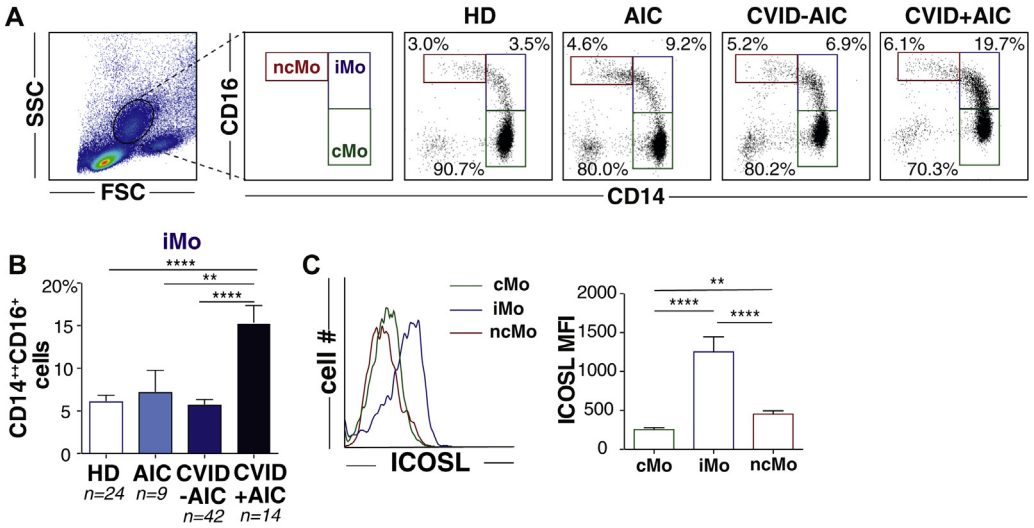

FIG 4. Monocytes from CVID+AIC subjects express increased ICOSL. **A,** Representative dot plot *(upper)* of classical monocytes (*cMo*; $CD14^{+}CD16^{-}$), intermediate monocytes (*iMo*; $CD14^{+}CD16^{+}$), and nonclassical monocytes (*ncMo*; $CD14^{int}CD16^{+}$). *FSC,* Forward scatter; *SSC,* side scatter. **B,** iMo frequencies in HDs, immunocompetent subjects with AICs, CVID−AIC subjects, and CVID+AIC subjects. **C,** ICOSL mean fluorescence intensities *(MFI)* on monocyte subsets from representative donors *(left)* and all subjects. $^{**}P < .01$ and $^{****}P < .0001$, Mann-Whitney *U* test.

samples from HDs, immunocompetent subjects with AICs, and CVID−AIC subjects (526, 791, and 904 pg/mL at $P < .0001$, $P < .001$, and $P < .05$, respectively; Fig 3, *D*), whereas concentrations of other T_{FH} cell–promoting cytokines, such as IL-12 and IL-6, were not different (see Fig E9 in this article's Online Repository at www.jacionline.org).[48,49,54] Furthermore, we found that activin A concentrations positively correlated with cT_{FH} cell frequencies in all analyzed subjects, regardless of their disease status ($r = 0.43$, $P < .0001$; Fig 3, *D*), and that serum IgA concentrations negatively correlated with both cT_{FH} cell frequencies ($r = -0.54$, $P < .001$) and plasma activin A concentrations ($r = -0.37$, $P < .01$; see Fig E10 in this article's Online Repository at www.jacionline.org).

In addition to promoting release of soluble mediators, such as activin A, endotoxin also induces ICOSL expression by antigen-presenting cells, including human monocytoid lines and monocyte-derived DCs.[55] To determine whether T_H cells from CVID+AIC subjects are more likely to encounter monocyte-expressed ICOSL *in vivo*, we surveyed different circulating monocyte subsets for ICOSL expression (Fig 4, *A*). In all subjects we found ICOSL to be primarily expressed on $CD14^{++}CD16^{+}$ intermediate monocytes (Fig 4, *C*), a population enlarged nearly 3-fold in blood samples from CVID+AIC subjects versus samples from CVID−AIC subjects, immunocompetent subjects with AICs, and HDs (15.6% vs 5.7%, 4.1%, and 6.1%, respectively; $P < .0001$ for each comparison; Fig 4, *B*, and see Figs E11 and E12 in this article's Online Repository at www.jacionline.org). The absolute number of ICOSL-expressing intermediate monocytes was also greatest in CVID+AIC subjects. Hence, either through a direct effect or through activin A/ICOSL induction, endotoxin promotes early T_H cell commitment to the follicular lineage.

cT_{FH} cells from CVID+AIC subjects provide efficient B-cell help

Unlike more phenotypically homogenous tonsillar T_{FH} cells, cT_{FH} cells exhibit more heterogeneous chemokine receptor expression, cytokine secretion, and functional profiles.[44,56] For instance, HD cT_{FH} cells can be divided into at least 2 distinct functional subsets: (1) a CXCR3-expressing, IFN-γ–secreting subset that does not provide efficient B-cell help and (2) a CXCR3-nonexpressing IL-21, IL-4, and IL-17 secreting subset that does (see Figs E13 and E14 in this article's Online Repository at www.jacionline.org).[56] Because CVID+AIC subjects are hypogammaglobulinemic yet also possess enlarged cT_{FH} pools (Fig 1, *C*, and see Fig E15 in this article's Online Repository at www.jacionline.org),[8] we sought to compare CXCR3 expression, cytokine secretion, and functionality of their cT_{FH} cells with counterparts from HDs, immunocompetent subjects with AICs, and CVID−AIC subjects whose cT_{FH} cell frequencies were not increased, even in the context of noncytopenic autoimmune diseases. Unlike cells from other subjects, which were equally divided between CXCR3-expressing and nonexpressing cells, cT_{FH} cells from CVID+AIC subjects uniformly and overwhelmingly (>90%) express $CXCR3^{+}$ ($P < .0001$ against all other subject groups; Fig 5, *A*).[20] Corresponding with increased $CXCR3^{+}$ cT_{FH} cell frequencies, samples from CVID+AIC subjects also contained significantly greater plasma concentrations of the CXCR3 ligands CXCL9, CXCL10, and CXCL11 (see Fig E16, *A*, in this article's Online Repository at www.jacionline.org). The CCR4 and CCR6 ligands CCL17 and CCL20 were not significantly different between subject groups (see Fig E16, *B*).

Despite near-universal CXCR3 expression, cT_{FH} cell transcriptomes from CVID+AIC subjects were significantly

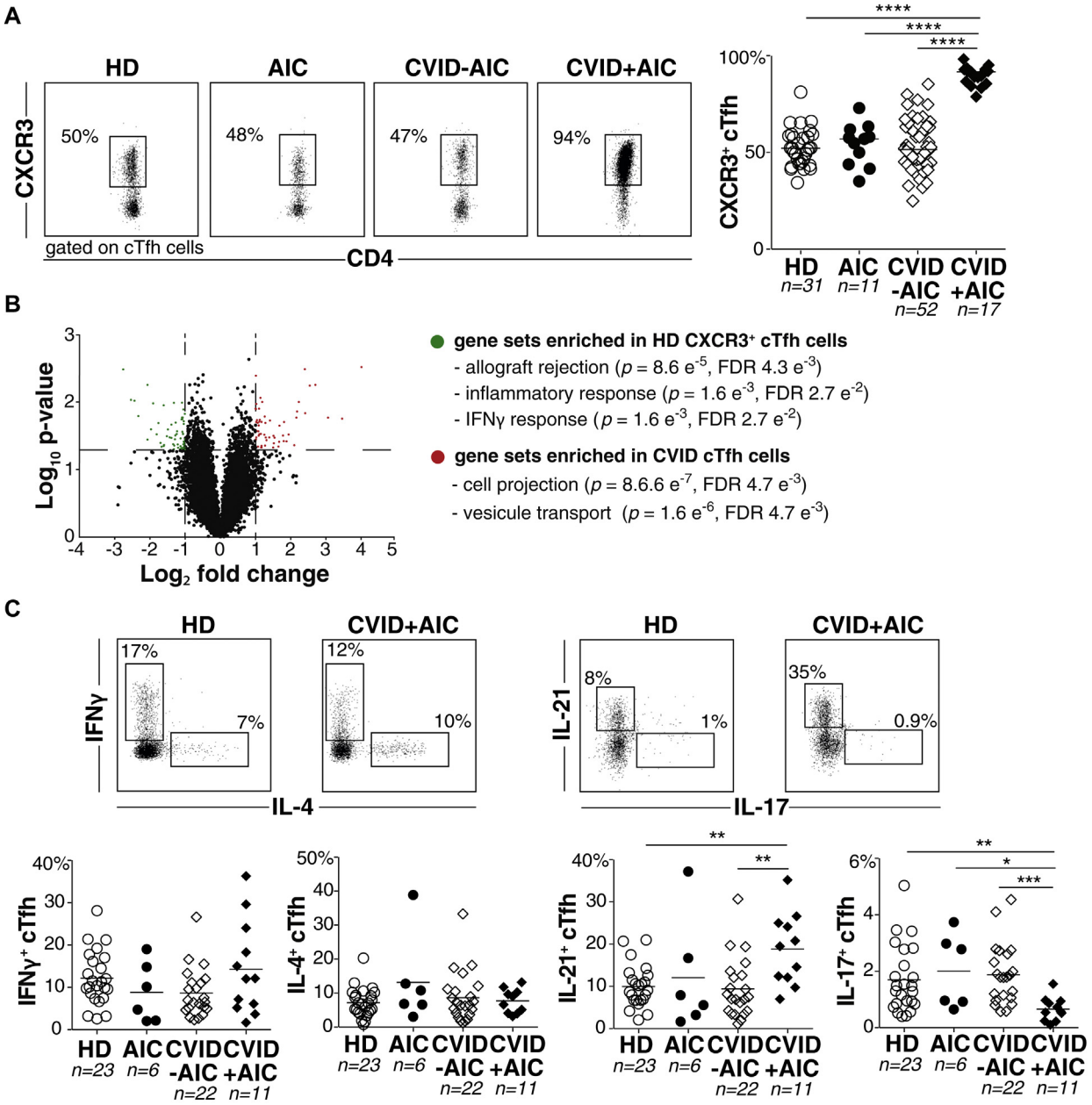

FIG 5. Most cT_{FH} cells from CVID+AIC subjects express $CXCR3^+$ but are functionally distinct from $CXCR3^+$ cT_{FH} cells from HDs. **A,** Frequencies of cT_{FH} cells expressing CXCR3 are displayed for representative subjects *(left)* and all available subjects, including immunocompetent subjects with AICs.[20] **B,** Differentially expressed transcripts between cT_{FH} cells from CVID+AIC subjects and $CXCR3^+$ cT_{FH} cells from HDs are displayed in a volcano plot, with enriched gene sets listed. *FDR,* False discovery rate. **C,** Frequency of activated cT_{FH} cells staining positive for intracellular cytokines are shown for representative subjects *(left)* and all available subjects. $*P < .05$, $**P < .01$, $***P < .001$, and $****P < .0001$, Mann-Whitney *U* test.

different from $CXCR3^+$ cT_{FH} cells from HDs and assorted separately when subjected to a hierarchical cluster analysis algorithm (see Fig E17 in this article's Online Repository at www.jacionline.org). Gene set enrichment analyses revealed cT_{FH} cells from CVID subjects had prominent anaerobic respiration and glycolysis signatures consistent with activation (data not shown). cT_{FH} cells from CVID+AIC subjects also lacked the inflammatory IFN-γ response transcriptional signature, which defined $CXCR3^+$ cT_{FH} cells from HDs (Fig 5, *B*), a finding consistent with nonincreased plasma IFN-γ concentrations in CVID+AIC subjects (see Fig E18 in this article's Online Repository at www.jacionline.org). Indeed, we found that cT_{FH} cells from CVID+AIC subjects did not exhibit the IFN-γ–dominant cytokine secretion profile characteristic of $CXCR3^+$ cT_{FH} cells from HDs (Fig 5, *C*). Instead, they expressed IL-21 at a frequency twice that of cT_{FH} cells from HDs and CVID−AIC subjects ($P < .01$ for both comparisons). Despite more IL-21, cT_{FH} cell cytokine secretion profiles from CVID+AIC subjects still

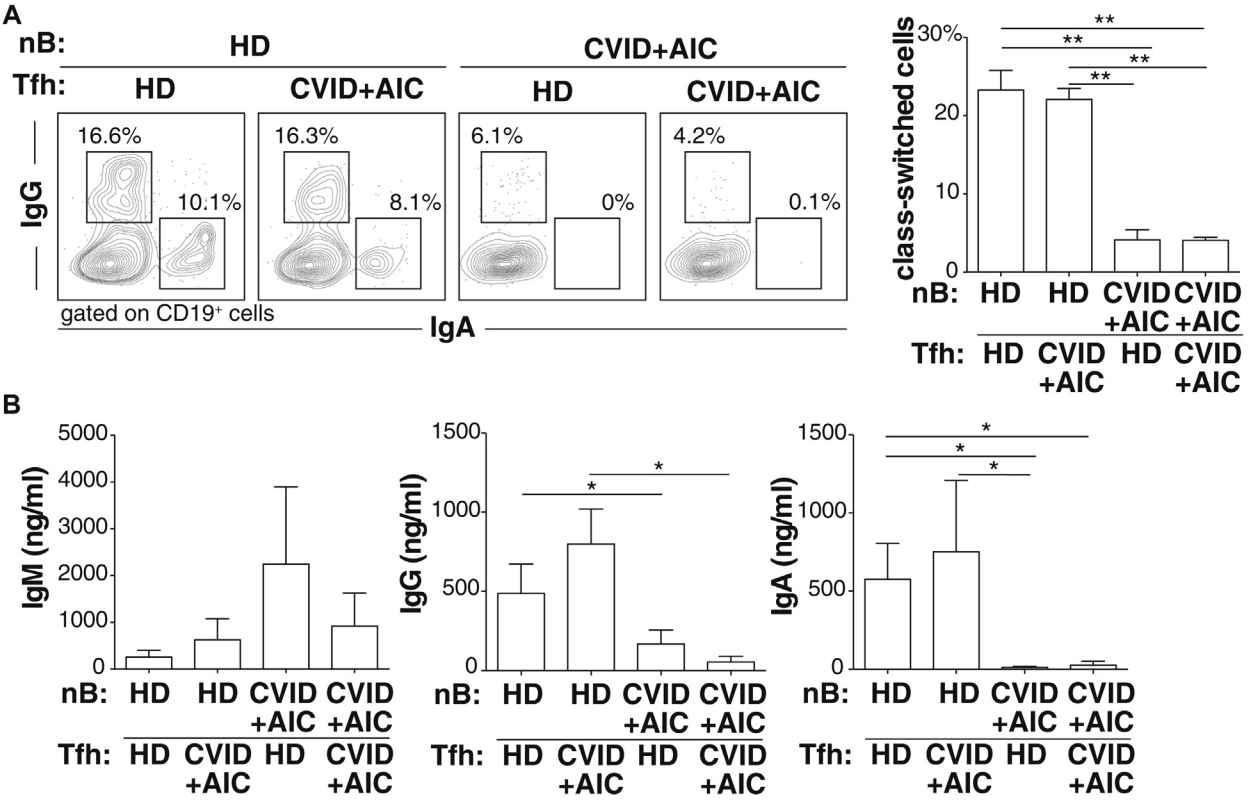

FIG 6. cT_{FH} cells from CVID subjects efficiently help receptive B cells. **A,** Day 7 IgG and IgA cell-surface expression frequencies on naive B cells *(nB)* from representative indicated subjects in homologous or heterologous cocultures with cT_{FH} cells from indicated subjects *(left)* and mean frequencies tallied from 4 separate experiments. **B,** Mean immunoglobulin concentrations in supernatants from the described cocultures are displayed. *Error bars* indicate means ± SEMs. **P* < .05 and ***P* < .01, Mann-Whitney *U* test.

differed from those of characteristic $CXCR3^-$ cT_{FH} cells. For instance, IL-4–secreting cT_{FH} cell frequencies were not different and IL-17–secreting cT_{FH} cell frequencies were significantly lower in cT_{FH} cells from CVID+AIC subjects than in cT_{FH} cells from HDs and CVID−AIC subjects.

Arguably, it is function and not surface markers or cytokine profiles that should arbitrate T_H cell identity. To determine whether cT_{FH} cells from CVID+AIC subjects are capable of providing B-cell help, we cocultured them with either heterologous naive B cells from HDs or homologous naive B cells from CVID+AIC subjects ($CD19^+CD21^+IgM^+CD27$). At day 7, we found cT_{FH} cells from CVID+AIC subjects were just as effective as cT_{FH} cells from HDs at inducing HD B-cell CSR and IgA/IgG secretion (Fig 6). In contrast, naive B cells from CVID+AIC subjects were generally unable to secrete class-switched antibodies irrespective of the cT_{FH} cell donor. Thus, despite near-unanimous $CXCR3^+$ expression, cT_{FH} cells from CVID+AIC subjects are primarily IL-21–secreting cells capable of providing efficient help to responsive B cells.

Circulating $CD25^{hi}CD127^{lo}CXCR5^+PD\text{-}1^+$ helper cells are not Treg cells

Our high-dimensional CyTOF analysis of 3 pooled samples from CVID+AIC subjects identified a unique population of $CD25^{hi}CD127^{lo}$ cells within the P3 gate that also expressed the T_{FH} cell makers ICOS, CXCR5, and PD-1 (Fig 1, *D*). To confirm this finding in our larger cohort and to further investigate this novel cell population, we analyzed follicular subsets contained within the $CD25^{hi}CD127^{lo/-}$ "Treg" cell gate by using FACS. We found HDs, CVID−AIC subjects, and immunocompetent subjects with AICs had 2 distinct subpopulations (Fig 7, *A*, and see Fig E19 in this article's Online Repository at www.jacionline.org). Both expressed the regulatory transcription factor FOXP3 (Fig 7, *B*) and suppressed HD T-effector cell proliferation *in vitro* (see Fig E20 in this article's Online Repository at www.jacionline.org). Only 1 expressed CXCR5 consistent with circulating follicular regulatory T cells (shown in green).[57] The $CXCR5^-$ population, which comprised approximately 75% of the $CD25^{hi}CD127^{lo}$ gate, corresponded to traditional Treg cells (gray).

CVID+AIC subjects possessed a third $CD25^{hi}CD127^{lo}$ subpopulation expressing CXCR5, PD-1, Ki67, ICOS, IL-21, and IL-10 (red; Fig 7, *B* and *C*, and see Fig E21, *A*, in this article's Online Repository at www.jacionline.org). The subpopulation comprised an average 12.4% of the "Treg" cell gate, a share gained primarily at the expense of circulating follicular regulatory T cells (Fig 7, *A*). Although highly expressing CD25, IL-10, and the inhibitory coreceptor molecule cytotoxic T lymphocyte–associated protein 4 (Fig 7, *C*, and see Fig E21, *B*), these cells did not stain positively for FOXP3 (Fig 7, *B*) and could not suppress effector T-cell proliferation *in vitro*

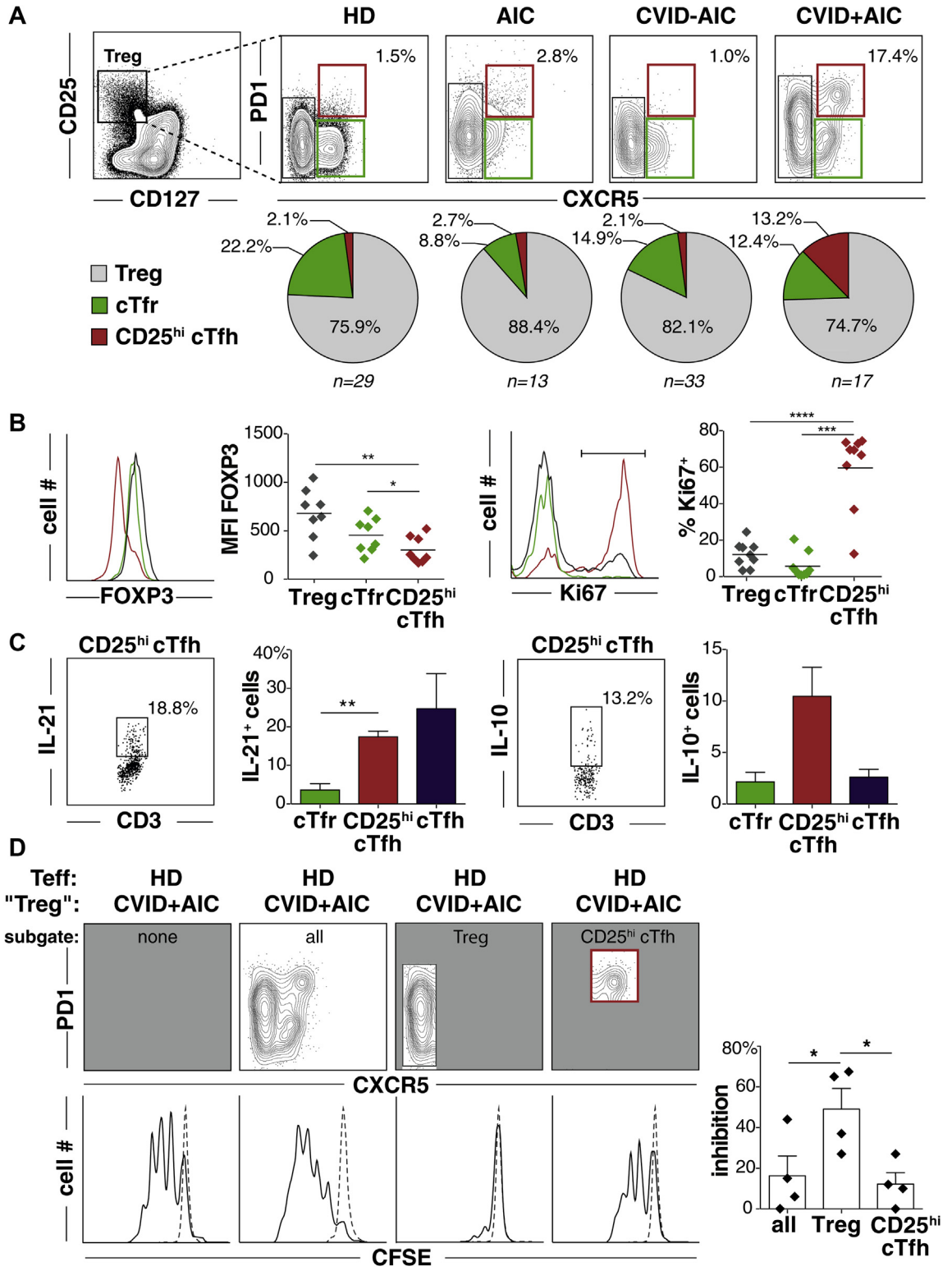

FIG 7. The $CD25^{hi}CD127^{lo}$ "Treg" cell gate in CVID+AIC subjects is contaminated by a poorly suppressive cT_{FH}-like cell subset. **A,** Peripheral $CD4^+$ cells in the $CD25^{hi}CD127^{lo/-}$ "Treg" cell gate include conventional Treg cells (gray), $CXCR5^+PD\text{-}1^{lo}$ circulating T follicular regulatory cells (*Tfr*, green), and a third $CXCR5^+PD\text{-}1^{hi}$ population, $CD25^{hi}$ T_{FH}-like cells (red). **B** and **C,** FOXP3 and Ki67 (Fig 6, *B*) and IL-21 and IL-10 (Fig 6, *C*) expression and expression frequencies on T-cell subsets from CVID+AIC subjects and HDs. *MFI,* Mean fluorescence intensity. **D,** Representative histograms *(left)* of CFSE-labeled HD naive T effector cells *(Teff)* stimulated *(solid line)* or not *(dashed line)* in cocultures with indicated T_H cell subsets from CVID+AIC subjects. Columns represent mean percentage inhibition relative to unstimulated Teff cells. *Error bars* indicate means ± SEMs. $*P < .05$, $**P < .01$, $***P < .001$, and $****P < .0001$, Mann-Whitney *U* test or paired *t* test.

(Fig 7, *D*). Furthermore, depletion of PD-1$^+$CXCR5$^+$ cells significantly improved the suppressive function of remaining FOXP3$^+$ cells from CVID+AIC subjects (Fig 7, *D*). Hence, although they highly express CD25 and do not express CD127, circulating CD25^{hi}CD127^{lo}CXCR5$^+$PD-1$^+$ T_H cells are not regulatory cells.

DISCUSSION

Here, using high-dimensional analysis, we systematically catalogued the phenotypic distribution of circulating CD4$^+$ T cells in CVID subjects. Our data establish CVID subjects in our cohort to display one of 2 immune phenotypes: either pure antibody deficiency without significant T_H cell effects (CVID−AIC subjects) or antibody deficiency, including undetectable serum IgA, complicated by the T cell–altering effects of systemic endotoxemia (CVID+AIC subjects).

Endotoxin's adjuvant properties were first described by Condie and Good in 1955[58] and were later attributed to direct TLR4-mediated mitogenic effects on murine B cells.[59,60] Because human B cells do not express TLR4, we think it unlikely that LPS exerts direct effects on B cells from CVID subjects.[61] Instead, our own *in vitro* data demonstrate that plasma endotoxin promotes a follicular program in naive T cells, a population known to express TLR4.[62] We propose the observed T_{FH} cell skewing effect of endotoxin might maintain antibody/microbial balance at mucosal surfaces in immunocompetent hosts but also might promote pathologic autoantibody production in antibody-deficient CVID subjects.

Although others have demonstrated a T_H1 but not a T_{FH} cell bias in LPS-exposed human T cells, our results are likely influenced by the additional *in vitro* effects of recombinant ICOSL. Induced by LPS[55] and expressed by an increased number of monocytes from CVID+AIC subjects, it is likely that endogenous ICOSL similarly promotes T_{FH} differentiation in CVID+AIC subjects *in vivo*.

Another protein induced by endotoxin[53] and highly concentrated in plasma from CVID+AIC subjects is the inflammatory protein activin A. Activin A was previously shown to be an elite T_{FH} lineage promoter in a high-throughput *in vitro* screen of more than 2000 human inflammatory proteins.[50] The strong correlations between cT_{FH} cell frequencies, plasma activin A concentrations, and serum IgA levels that we report here provide the first *in vivo* proof of this concept in a human disease.

Several CVID-related T_H cell phenomena found by our analyses were previously observed in more narrowly focused studies. Our intentionally broader approach provides us the opportunity to both corroborate earlier findings and, in some cases, reinterpret them aided by additional contextual clues. For instance, reduced naive T-cell frequencies and T-cell receptor excision circle concentrations in CVID subjects were previously thought to signal poor thymic output,[23-25] yet our data indicate RTEs from CVID+AIC subjects are likely scarce because they leave the thymus in a preactivated state, favoring proliferation and accelerated differentiation. Similarly, it was recently proposed but not demonstrated in cocultures that increased CXCR3 expression by cT_{FH} cells from CVID subjects was the cause of traditional CVID B-cell defects in CSR, somatic hypermutation, and memory B-cell formation.[27] Although we also found increased frequencies of CXCR3-expressing cT_{FH} cells in CVID+AIC subjects, in our hands these cells are primarily IL-21 but not IFN-γ producers that are as effective at promoting *in vitro* class-switched antibody production as cT_{FH} cells from HDs. Furthermore, instead of predicting poor helper function, we find CXCR3 expression on T_{FH} cells from CVID+AIC subjects to instead correlate with stark IgA deficiency and endotoxin-induced release of the CXCR3 ligands CXCL9, CXCL10, and CXCL11 from innate cells.[63-67] Thus, other than a few notable exceptions,[22,68,69] CVID-related hypogammaglobulinemia appears primarily attributable to intrinsically unresponsive B cells and not to T_{FH} cell dysfunction. Although it is possible that IFN-γ–producing cT_{FH} cells can predominate in other cohorts with CVID more enriched with granulomatous diseases than ours,[27,70] our data clearly demonstrate that cT_{FH} cell function cannot be intuited from chemokine receptor expression alone, especially in immunodeficient subjects.

Finally, previous reports, including our own, demonstrate CD25^{hi}CD127$^-$ "Treg" cells from CVID subjects perform poorly in traditional *in vitro* suppression assays.[3,8,26] Here we demonstrate that this phenomenon is unlikely caused by Treg cell intrinsic defects but is instead secondary to contamination of the traditional human "Treg" cell sorting gate with CD25^{hi} cT_{FH}-like cells. A notable exception might be truly dysfunctional cytotoxic T lymphocyte–associated protein 4–haploinsufficient or LRBA-deficient Treg cells that poorly suppress,[71,72] even when depleted of CD25^{hi} cT_{FH} cells.[73] In all cases, especially in CVID subjects, CXCR5$^+$PD-1$^+$ cells, including CD25^{hi} cT_{FH}-like cells, should be excluded from *in vitro* Treg cell suppression assays to avoid confounding effects. The biologic role of the IL-10–producing CD25^{hi} cT_{FH}-like cells described here is currently unclear, but phenotypically similar cells with regulatory function were recently described in human tonsils.[74] The remarkable expansion of the circulating CD25^{hi} cT_{FH}-like cells we describe here suggests they are pathologically linked to autoantibody production. Identification, localization, and functional investigation of tissue-resident counterparts to circulating CD25^{hi} cT_{FH}-like cells in the secondary lymphoid tissues of HDs and CVID subjects will be critical to understanding whether and how they influence disease pathogenesis.

We are very much indebted to the subjects. We thank John Tobias, PhD, of the University of Pennsylvania Genomic Analysis Core for assistance with biostatistical analyses.

Key messages

- **Endotoxin promotes T_{FH} cell differentiation *in vitro*.**
- **T_{FH} cells from CVID subjects can help receptive HD B cells secrete class-switched immunoglobulins.**
- **Treg cells from many CVID subjects are suppressive if CD25$^+$ T_{FH}-like cells are excluded from *in vitro* assays.**

REFERENCES

1. Cunningham-Rundles C. The many faces of common variable immunodeficiency. Hematol Am Soc Hematol Educ Program 2012;2012:301-5.
2. Romberg N, Cunningham-Rundles C, Meffre E. Response: common variable immunodeficiency patients with increased CD21−/lo B cells suffer from altered receptor editing and defective central B-cell tolerance. Blood 2011;118:5977-8.

3. Romberg N, Chamberlain N, Saadoun D, Gentile M, Kinnunen T, Ng YS, et al. CVID-associated TACI mutations affect autoreactive B cell selection and activation. J Clin Invest 2013;123:4283-93.
4. Simchoni N, Cunningham-Rundles C. TLR7- and TLR9-responsive human B cells share phenotypic and genetic characteristics. J Immunol 2015;194:3035-44.
5. Yu JE, Knight AK, Radigan L, Marron TU, Zhang L, Sanchez-Ramon S, et al. Toll-like receptor 7 and 9 defects in common variable immunodeficiency. J Allergy Clin Immunol 2009;124:349-56.e1-3.
6. Castigli E, Geha RS. Molecular basis of common variable immunodeficiency. J Allergy Clin Immunol 2006;117:740-7.
7. Warnatz K, Denz A, Drager R, Braun M, Groth C, Wolff-Vorbeck G, et al. Severe deficiency of switched memory B cells (CD27(+)IgM(-)IgD(-)) in subgroups of patients with common variable immunodeficiency: a new approach to classify a heterogeneous disease. Blood 2002;99:1544-51.
8. Romberg N, Le Coz C, Glauzy S, Schickel JN, Trofa M, Nolan BE, et al. Patients with common variable immunodeficiency with autoimmune cytopenias exhibit hyperplastic yet inefficient germinal center responses. J Allergy Clin Immunol 2019;143:258-65.
9. Roskin KM, Simchoni N, Liu Y, Lee JY, Seo K, Hoh RA, et al. IgH sequences in common variable immune deficiency reveal altered B cell development and selection. Sci Transl Med 2015;7:302ra135.
10. Almejun MB, Campos BC, Patino V, Galicchio M, Zelazko M, Oleastro M, et al. Noninfectious complications in patients with pediatric-onset common variable immunodeficiency correlated with defects in somatic hypermutation but not in class-switch recombination. J Allergy Clin Immunol 2017;139:913-22.
11. Ochtrop ML, Goldacker S, May AM, Rizzi M, Draeger R, Hauschke D, et al. T and B lymphocyte abnormalities in bone marrow biopsies of common variable immunodeficiency. Blood 2011;118:309-18.
12. Perreau M, Vigano S, Bellanger F, Pellaton C, Buss G, Comte D, et al. Exhaustion of bacteria-specific CD4 T cells and microbial translocation in common variable immunodeficiency disorders. J Exp Med 2014;211:2033-45.
13. Kuehn HS, Boisson B, Cunningham-Rundles C, Reichenbach J, Stray-Pedersen A, Gelfand EW, et al. Loss of B Cells in Patients with Heterozygous Mutations in IKAROS. N Engl J Med 2016;374:1032-43.
14. Warnatz K, Salzer U, Rizzi M, Fischer B, Gutenberger S, Bohm J, et al. B-cell activating factor receptor deficiency is associated with an adult-onset antibody deficiency syndrome in humans. Proc Natl Acad Sci U S A 2009;106:13945-50.
15. Chen K, Coonrod EM, Kumanovics A, Franks ZF, Durtschi JD, Margraf RL, et al. Germline mutations in NFKB2 implicate the noncanonical NF-kappaB pathway in the pathogenesis of common variable immunodeficiency. Am J Hum Genet 2013;93:812-24.
16. Kuehn HS, Niemela JE, Sreedhara K, Stoddard JL, Grossman J, Wysocki CA, et al. Novel nonsense gain-of-function NFKB2 mutations associated with a combined immunodeficiency phenotype. Blood 2017;130:1553-64.
17. van Zelm MC, Smet J, Adams B, Mascart F, Schandene L, Janssen F, et al. CD81 gene defect in humans disrupts CD19 complex formation and leads to antibody deficiency. J Clin Invest 2010;120:1265-74.
18. de Valles-Ibanez G, Esteve-Sole A, Piquer M, Gonzalez-Navarro EA, Hernandez-Rodriguez J, Laayouni H, et al. Evaluating the genetics of common variable immunodeficiency: monogenetic model and beyond. Front Immunol 2018;9:636.
19. Fliegauf M, Bryant VL, Frede N, Slade C, Woon ST, Lehnert K, et al. Haploinsufficiency of the NF-kappaB1 subunit p50 in common variable immunodeficiency. Am J Hum Genet 2015;97:389-403.
20. Thiel J, Kimmig L, Salzer U, Grudzien M, Lebrecht D, Hagena T, et al. Genetic CD21 deficiency is associated with hypogammaglobulinemia. J Allergy Clin Immunol 2012;129:801-10.e6.
21. Alkhairy OK, Perez-Becker R, Driessen GJ, Abolhassani H, van Montfrans J, Borte S, et al. Novel mutations in TNFRSF7/CD27: clinical, immunologic, and genetic characterization of human CD27 deficiency. J Allergy Clin Immunol 2015;136:703-12.e10.
22. Salzer E, Kansu A, Sic H, Majek P, Ikinciogullari A, Dogu FE, et al. Early-onset inflammatory bowel disease and common variable immunodeficiency-like disease caused by IL-21 deficiency. J Allergy Clin Immunol 2014;133:1651-9.e12.
23. De Vera MJ, Al-Harthi L, Gewurz AT. Assessing thymopoiesis in patients with common variable immunodeficiency as measured by T-cell receptor excision circles. Ann Allergy Asthma Immunol 2004;93:478-84.
24. Isgro A, Marziali M, Mezzaroma I, Luzi G, Mazzone AM, Guazzi V, et al. Bone marrow clonogenic capability, cytokine production, and thymic output in patients with common variable immunodeficiency. J Immunol 2005;174:5074-81.
25. Guazzi V, Aiuti F, Mezzaroma I, Mazzetta F, Andolfi G, Mortellaro A, et al. Assessment of thymic output in common variable immunodeficiency patients by evaluation of T cell receptor excision circles. Clin Exp Immunol 2002;129:346-53.
26. Yu GP, Chiang D, Song SJ, Hoyte EG, Huang J, Vanishsarn C, et al. Regulatory T cell dysfunction in subjects with common variable immunodeficiency complicated by autoimmune disease. Clin Immunol 2009;131:240-53.
27. Unger S, Seidl M, van Schouwenburg P, Rakhmanov M, Bulashevska A, Frede N, et al. The TH1 phenotype of follicular helper T cells indicates an IFN-gamma-associated immune dysregulation in patients with CD21low common variable immunodeficiency. J Allergy Clin Immunol 2018;141:730-40.
28. Conley ME, Notarangelo LD, Etzioni A. Diagnostic criteria for primary immunodeficiencies. Representing PAGID (Pan-American Group for Immunodeficiency) and ESID (European Society for Immunodeficiencies). Clin Immunol 1999;93:190-7.
29. Rodeghiero F, Stasi R, Gernsheimer T, Michel M, Provan D, Arnold DM, et al. Standardization of terminology, definitions and outcome criteria in immune thrombocytopenic purpura of adults and children: report from an international working group. Blood 2009;113:2386-93.
30. Neunert C, Lim W, Crowther M, Cohen A, Solberg L Jr, Crowther MA, et al. The American Society of Hematology 2011 evidence-based practice guideline for immune thrombocytopenia. Blood 2011;117:4190-207.
31. Lambert MP, Gernsheimer TB. Clinical updates in adult immune thrombocytopenia. Blood 2017;129:2829-35.
32. Aladjidi N, Leverger G, Leblanc T, Picat MQ, Michel G, Bertrand Y, et al. New insights into childhood autoimmune hemolytic anemia: a French national observational study of 265 children. Haematologica 2011;96:655-63.
33. Michel M, Chanet V, Dechartres A, Morin AS, Piette JC, Cirasino L, et al. The spectrum of Evans syndrome in adults: new insight into the disease based on the analysis of 68 cases. Blood 2009;114:3167-72.
34. Bousfiha A, Jeddane L, Picard C, Ailal F, Bobby Gaspar H, Al-Herz W, et al. The 2017 IUIS phenotypic classification for primary immunodeficiencies. J Clin Immunol 2018;38:129-43.
35. Bengsch B, Ohtani T, Khan O, Setty M, Manne S, O'Brien S, et al. Epigenomic-guided mass cytometry profiling reveals disease-specific features of exhausted CD8 T cells. Immunity 2018;48:1029-45. e5.
36. van der Maaten LJP, Hinton GE. Visualizing high-dimensional data using t-SNE. J Machine Learning Res 2008;9:2579-605.
37. Van Gassen S, Callebaut B, Van Helden MJ, Lambrecht BN, Demeester P, Dhaene T, et al. FlowSOM: Using self-organizing maps for visualization and interpretation of cytometry data. Cytometry A 2015;87:636-45.
38. Mootha VK, Lindgren CM, Eriksson KF, Subramanian A, Sihag S, Lehar J, et al. PGC-1alpha-responsive genes involved in oxidative phosphorylation are coordinately downregulated in human diabetes. Nat Genet 2003;34:267-73.
39. Subramanian A, Tamayo P, Mootha VK, Mukherjee S, Ebert BL, Gillette MA, et al. Gene set enrichment analysis: a knowledge-based approach for interpreting genome-wide expression profiles. Proc Natl Acad Sci U S A 2005;102:15545-50.
40. Choi YS, Kageyama R, Eto D, Escobar TC, Johnston RJ, Monticelli L, et al. ICOS receptor instructs T follicular helper cell versus effector cell differentiation via induction of the transcriptional repressor Bcl6. Immunity 2011;34:932-46.
41. Choi YS, Gullicksrud JA, Xing S, Zeng Z, Shan Q, Li F, et al. LEF-1 and TCF-1 orchestrate T(FH) differentiation by regulating differentiation circuits upstream of the transcriptional repressor Bcl6. Nat Immunol 2015;16:980-90.
42. Breitfeld D, Ohl L, Kremmer E, Ellwart J, Sallusto F, Lipp M, et al. Follicular B helper T cells express CXC chemokine receptor 5, localize to B cell follicles, and support immunoglobulin production. J Exp Med 2000;192:1545-52.
43. Schaerli P, Willimann K, Lang AB, Lipp M, Loetscher P, Moser B. CXC chemokine receptor 5 expression defines follicular homing T cells with B cell helper function. J Exp Med 2000;192:1553-62.
44. Morita R, Schmitt N, Bentebibel SE, Ranganathan R, Bourdery L, Zurawski G, et al. Human blood CXCR5(+)CD4(+) T cells are counterparts of T follicular cells and contain specific subsets that differentially support antibody secretion. Immunity 2011;34:108-21.
45. Ballesteros-Tato A, Leon B, Graf BA, Moquin A, Adams PS, Lund FE, et al. Interleukin-2 inhibits germinal center formation by limiting T follicular helper cell differentiation. Immunity 2012;36:847-56.
46. Liu W, Putnam AL, Xu-Yu Z, Szot GL, Lee MR, Zhu S, et al. CD127 expression inversely correlates with FoxP3 and suppressive function of human CD4+ T reg cells. J Exp Med 2006;203:1701-11.
47. Kimmig S, Przybylski GK, Schmidt CA, Laurisch K, Mowes B, Radbruch A, et al. Two subsets of naive T helper cells with distinct T cell receptor excision circle content in human adult peripheral blood. J Exp Med 2002;195:789-94.
48. Schmitt N, Morita R, Bourdery L, Bentebibel SE, Zurawski SM, Banchereau J, et al. Human dendritic cells induce the differentiation of interleukin-21-producing T follicular helper-like cells through interleukin-12. Immunity 2009;31:158-69.
49. Eto D, Lao C, DiToro D, Barnett B, Escobar TC, Kageyama R, et al. IL-21 and IL-6 are critical for different aspects of B cell immunity and redundantly induce optimal follicular helper CD4 T cell (Tfh) differentiation. PLoS One 2011;6:e17739.
50. Locci M, Wu JE, Arumemi F, Mikulski Z, Dahlberg C, Miller AT, et al. Activin A programs the differentiation of human TFH cells. Nat Immunol 2016;17:976-84.

51. Dong C, Juedes AE, Temann UA, Shresta S, Allison JP, Ruddle NH, et al. ICOS co-stimulatory receptor is essential for T-cell activation and function. Nature 2001;409:97-101.
52. Jacquemin C, Schmitt N, Contin-Bordes C, Liu Y, Narayanan P, Seneschal J, et al. OX40 ligand contributes to human lupus pathogenesis by promoting T follicular helper response. Immunity 2015;42:1159-70.
53. Jones KL, Mansell A, Patella S, Scott BJ, Hedger MP, de Kretser DM, et al. Activin A is a critical component of the inflammatory response, and its binding protein, follistatin, reduces mortality in endotoxemia. Proc Natl Acad Sci U S A 2007; 104:16239-44.
54. Ma CS, Suryani S, Avery DT, Chan A, Nanan R, Santner-Nanan B, et al. Early commitment of naive human CD4(+) T cells to the T follicular helper (T(FH)) cell lineage is induced by IL-12. Immunol Cell Biol 2009;87:590-600.
55. Hedl M, Lahiri A, Ning K, Cho JH, Abraham C. Pattern recognition receptor signaling in human dendritic cells is enhanced by ICOS ligand and modulated by the Crohn's disease ICOSLG risk allele. Immunity 2014;40:734-46.
56. Locci M, Havenar-Daughton C, Landais E, Wu J, Kroenke MA, Arlehamn CL, et al. Human circulating PD-1+CXCR3-CXCR5+ memory Tfh cells are highly functional and correlate with broadly neutralizing HIV antibody responses. Immunity 2013;39:758-69.
57. Fonseca VR, Agua-Doce A, Maceiras AR, Pierson W, Ribeiro F, Romao VC, et al. Human blood Tfr cells are indicators of ongoing humoral activity not fully licensed with suppressive function. Sci Immunol 2017;2.
58. Condie RM, Zak SJ, Good RA. Effect of meningococcal endotoxin on the immune response. Proc Soc Exp Biol Med 1955;90:355-60.
59. Andersson J, Melchers F, Galanos C, Luderitz O. The mitogenic effect of lipopolysaccharide on bone marrow-derived mouse lymphocytes. Lipid A as the mitogenic part of the molecule. J Exp Med 1973;137:943-53.
60. Lutzker S, Rothman P, Pollock R, Coffman R, Alt FW. Mitogen- and IL-4-regulated expression of germ-line Ig gamma 2b transcripts: evidence for directed heavy chain class switching. Cell 1988;53:177-84.
61. Hornung V, Rothenfusser S, Britsch S, Krug A, Jahrsdorfer B, Giese T, et al. Quantitative expression of toll-like receptor 1-10 mRNA in cellular subsets of human peripheral blood mononuclear cells and sensitivity to CpG oligodeoxynucleotides. J Immunol 2002;168:4531-7.
62. Komai-Koma M, Jones L, Ogg GS, Xu D, Liew FY. TLR2 is expressed on activated T cells as a costimulatory receptor. Proc Natl Acad Sci U S A 2004; 101:3029-34.
63. Widney DP, Xia YR, Lusis AJ, Smith JB. The murine chemokine CXCL11 (IFN-inducible T cell alpha chemoattractant) is an IFN-gamma- and lipopolysaccharide-inducible glucocorticoid-attenuated response gene expressed in lung and other tissues during endotoxemia. J Immunol 2000;164:6322-31.
64. Loos T, Dekeyzer L, Struyf S, Schutyser E, Gijsbers K, Gouwy M, et al. TLR ligands and cytokines induce CXCR3 ligands in endothelial cells: enhanced CXCL9 in autoimmune arthritis. Lab Invest 2006;86:902-16.
65. Herzig DS, Driver BR, Fang G, Toliver-Kinsky TE, Shute EN, Sherwood ER. Regulation of lymphocyte trafficking by CXC chemokine receptor 3 during septic shock. Am J Respir Crit Care Med 2012;185:291-300.
66. Herzig DS, Luan L, Bohannon JK, Toliver-Kinsky TE, Guo Y, Sherwood ER. The role of CXCL10 in the pathogenesis of experimental septic shock. Crit Care 2014;18:R113.
67. Lang S, Li L, Wang X, Sun J, Xue X, Xiao Y, et al. CXCL10/IP-10 Neutralization can ameliorate lipopolysaccharide-induced acute respiratory distress syndrome in rats. PLoS One 2017;12:e0169100.
68. Bossaller L, Burger J, Draeger R, Grimbacher B, Knoth R, Plebani A, et al. ICOS deficiency is associated with a severe reduction of CXCR5+CD4 germinal center Th cells. J Immunol 2006;177:4927-32.
69. Ma CS, Wong N, Rao G, Avery DT, Torpy J, Hambridge T, et al. Monogenic mutations differentially affect the quantity and quality of T follicular helper cells in patients with human primary immunodeficiencies. J Allergy Clin Immunol 2015;136:993-1006.e1.
70. Park J, Munagala I, Xu H, Blankenship D, Maffucci P, Chaussabel D, et al. Interferon signature in the blood in inflammatory common variable immune deficiency. PLoS One 2013;8:e74893.
71. Kuehn HS, Ouyang W, Lo B, Deenick EK, Niemela JE, Avery DT, et al. Immune dysregulation in human subjects with heterozygous germline mutations in CTLA4. Science 2014;345:1623-7.
72. Charbonnier LM, Janssen E, Chou J, Ohsumi TK, Keles S, Hsu JT, et al. Regulatory T-cell deficiency and immune dysregulation, polyendocrinopathy, enteropathy, X-linked-like disorder caused by loss-of-function mutations in LRBA. J Allergy Clin Immunol 2015;135:217-27.
73. Le Coz C, Nolan BE, Trofa M, Kamsheh AM, Khokha MK, Lakhani SA, et al. Cytotoxic T-lymphocyte-associated protein 4 haploinsufficiency-associated inflammation can occur independently of T-cell hyperproliferation. Front Immunol 2018;9:1715.
74. Canete PF, Sweet RA, Gonzalez-Figueroa P, Papa I, Ohkura N, Bolton H, et al. Regulatory roles of IL-10-producing human follicular T cells. J Exp Med 2019; 216:1843-56.